Journal of Thermal Analysis, Vol. 47 (1996) 35-49

POLYMERIZATION KINETICS OF ACRYLIC BONE CEMENTS BY DIFFERENTIAL SCANNING CALORIMETRY

A. Maffezzoli

Department of Materials Science, University of Lecce, Via per Arnesano, 73100, Lecce, Italy

Abstract

Bone cements are widely used for the fixation of metallic prostheses in orthopaedics and to form replacements for skull defects in neurosurgery. Acrylic bone cements are based on a mixture of methyl methacrylate (MMA) and a fine powder of polymethyl methacrylate (PMMA). The polymerization of the bone cement occurs in contact with the bone and the prosthesis which act as the boundaries of a bulk polymerization reactor. The kinetic behaviour of the bone cement plays a fundamental role for the final performance of the implant.

In this paper, the isothermal and non-isothermal polymerization behaviour of a commercial bone cement is described. A simple phenomenological model, accounting for the autoacceleration effect, for a diffusion controlled termination mechanism and for the reaction between inhibitor and initiator, is proposed. The reaction kinetics is analysed by DSC. DSC data are used for the determination of the rates of polymerization under isothermal and non-isothermal conditions. The experimental data are processed to calculate the parameters of the proposed phenomenological kinetic model. The analytical and numerical details related to the integration of the model are discussed.

Keywords: bone cement, DSC, kinetics

Introduction

The fixation of metallic prostheses in orthopaedics and the restoration of skull defects in neurosurgery are usually achieved by poly(methyl methacrylate)-based bone cements which polymerize 'in situ' [1]. In the case of a total hip replacement, the bone cement, inserted in a femoral axial cavity appropriately drilled by the surgeon, acts as a bonding agent between the prosthesis and the bone. Acrylic bone cements are based on a mixture of methyl methacrylate (MMA) and a large fraction of a polymeric fine powder of polymethyl methacrylate (PMMA) and/or polystyrene (PS). Barium sulphate is often added in small fractions in order to obtain a radiopaque material. The liquid MMA and the solid polymeric powder are mixed by the surgeon and inserted in the bone cavity where the polymerization reaction occurs. During its application, the bone and the prosthesis act as the boundaries of a bulk polymerization reac-

0368–4466/96/ $ 5.00

John Wiley & Sons, Limited
Chichester

tor. As a consequency of the development of significant heat due to the exothermic nature of the polymerization reaction, a fast and highly non-isothermal bulk polymerization occurs. Furthermore, incomplete polymerization occurring in normal operative conditions may result in high levels of unreacted monomers in the cement. The residual MMA, slowly released from the cement, may be responsible for tissue damages. Tissue necrosis, caused by chemical or thermal causes effects, is a key factor for a good adhesion between the bone and the cement. For these reasons the properties and the performances of methyl methacrylate (MMA)-based bone cements are strongly dependent on their polymerization kinetics.

Furthermore, the peculiar characteristics of the polymerization environment require a short time for the completion of the reaction (typically 10–15 min at the body temperature) [1]. The initiation of the polymerization at low temperature is achieved by using a redox system such as amine-peroxide. The addition of a tertiary amine to peroxide initiators may increase the rate of production of radicals by several orders of magnitude at temperature lower then 50°C [2].

Bulk polymerization of MMA is greatly affected by diffusion at low and high values of the degree of reaction. In the first case, formation of high molecular weight molecules is responsible for a reduction in mobility of the chain end radicals resulting in a dramatic increase in the rate or reaction ('autoacceleration effect' or 'gel effect'). In the second case, the transition from a high-viscosity rubbery polymer to a glassy polymer (vitrification), strongly affects the polymerization kinetics causing the reaction to stop. In fact, the glass transition temperature, continuously increasing during cure, approaches the isothermal cure temperature thereby strongly reducing the molecular mobility. Under these conditions, the reaction becomes diffusion controlled and the termination step of the polymerization is governed by the strong reduction in the molecular mobility caused by vitrification [3–5].

Although the bulk polymerization of MMA has been widely studied [3, 6–10], the polymerization kinetics of bone cements is characterised by unique features as a consequence of the diffusion effects induced by the high fraction of polymeric filler. The addition of a solid polymer to the reactive medium enhances the rate of reaction acting on the onset of the so-called 'autoacceleration effect' or 'gel effect' [2, 3, 8, 10]. The autoacceleration effect is related to the viscosity of the reactive medium and can be observed at higher degrees of reaction when a non-reactive solvent is added to the monomer [2]. On the other hand, the higher the amount of polymeric filler added to the monomer the lower the onset temperature of the autoacceleration effect [9]. These experimental results indicate that the added polymer and the polymer formed during polymerization act in an equivalent way on the onset of the autoacceleration effect. Therefore the autoacceleration effect is exploited in the bone cements in order to decrease the reaction time, by inducing an accelerated reaction kinetics compared with pure MMA.

It must be underlined that the high rates of reaction observed are responsible for a fast heat generation that can cause high temperatures in contact with living tissues [11, 12]. Although the addition of solid polymer reduces the amount of heat generated by the reaction per unit mass of cement, the time during which this heat is released is very short, giving rise to temperatures between 50 and 108°C in contact with the bone [1].

In this work the reactive behaviour of a commercial bone cement was studied. The reaction kinetics was analysed using a simple phenomenological model accounting for the effects of autoacceleration and vitrification. The presence of the inhibitor was taken into account using a characteristic time of the reaction between initiator and inhibitor. Experimental data and model results were compared under isothermal and non-isothermal conditions. The analytical and numerical details related to the integration of the model are discussed.

Experimental

A commercial radiopaque bone cement, Surgical Simplex P, kindly supplied by Howmedica, was analysed. The powder and the liquid monomer, whose composition is given in Table 1, were mixed, according to the instructions of the supplier (20 ml of monomer and 40 g of powder).

Table 1 Composition of the studied material

Powder	Composition by weight
Poly methyl methacrylate (ρ =1.1 g cm^{-3})	15%
Methyl methacrylate-styrene copolymer (ρ =1.1 g cm^{-3})	75%
Barium sulphate U. S. P.	10%
Initiator (probably benzoyle peroxide (M_W =242)	(2018%?)

Liquid monomer	Composition by volume
Methyl methacrylate (M_W = 100, ρ =0.936 g cm^{-3})	97.4%
N,N-dimethyl para toluidine (M_W =135, ρ =0.936 g cm^{-3})	2.6%
Hydroquinone (M_W = 110, ρ =1.332 g cm^{-3})	75±15 ppm

Calorimetric analysis was carried out with a differential scanning calorimeter, Mettler DSC 30, operating with a constant nitrogen flow of 100 cm^3 min^{-1}. The sample preparation (6–10 mg) was performed at 20°C using a constant mixing time of 1.5 min. The overall handling time at 20°C, from the contact of the monomer with the powder (i.e. with the initiator) to the beginning of the DSC test was 2.5 min. The samples, weighed after each experiment, showed a negligible loss of monomer (less than 0.2 mg).

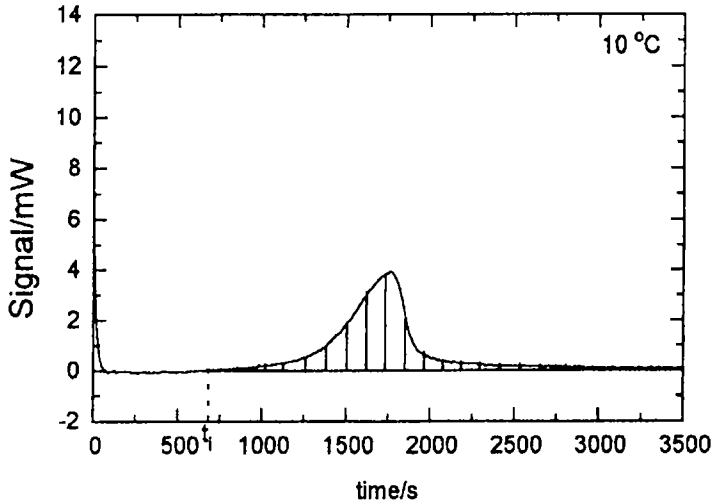

Fig. 1 Isothermal DSC curve obtained during polymerization at 10°C

Results and discussion

Initiation and inhibition

A typical DSC curve obtained for the studied materials at 10°C is presented in Fig. 1. The delay in the DSC signal represents an induction time (t_i), a relevant parameter from a processing point of view, associated with the reaction between initiator and inhibitor (hydroquinone) [13]. The amount of hydroquinone present in the cement is limited by its toxicity [1]. This reaction, started during mixing, delays the onset of the polymerization reaction by a time interval essential for the insertion of the cement and positioning of the prosthesis. For the thermal decomposition of a peroxide, the kinetics can be described by an exponential decay as a function of time [2], t:

$$[I] = [I_o]\exp(-K_d t) \tag{1}$$

where $[I]$ represents the concentration of initiator and K_d the kinetic constant. When an amine-peroxide system is used, the reaction of one mole of peroxide with one mole of amine leads to the production of one radical. Then, if stoichiometric proportions are used, a second order reaction kinetics is expected:

$$[P] = \frac{[P]}{1 + [P_o]K_d t} \tag{2}$$

where [P] represents the concentration of peroxide or amine. The reaction between initiator radicals and inhibitor may be analysed following the treatment of Fan and Lee [14]. If [I_z] is the concentration of initiator after all the inhibitor has been consumed:

$$q[Z_o] = f([I_o] - [I_Z]) \tag{3}$$

where [Z_o] and [I_o] are the initial concentrations of the inhibitor and initiator, respectively and q and f their efficiencies. When [I]=[I_z], the reaction starts and an exothermal DSC signal is observed after an induction time, t_i. By inserting Eqs (1–3), the following expressions are obtained:

$$K_d t_i = \left[- \ln \left(\frac{2f[I_o] - q[Z_o]}{2f[I_o]} \right) \right] \tag{4}$$

$$K_d t_i = \frac{1}{[P_o]} \left[\left(\frac{f[P_o]}{f[P_o] - q[Z_o]} \right) - 1 \right] \tag{5}$$

The factor 2 in Eq. (4) takes into account that the thermal decomposition of a peroxide produces two active radicals while the amine-peroxide reaction produces only one active radical. The induction time is the only macroscopic parameter representative of this reaction that can be detected by DSC. Hence, from these expressions, the kinetic constant of the initiation reaction may be calculated.

Furthermore, the temperature dependence of t_i may be used for the calculation of the activation energy (E_d) of the initiation reaction:

$$t_i = 1/[K_{ti} \exp(-E_d/RT)] \tag{6}$$

where K_{ti} is a function of the pre-exponential factor (K_{do}), the initiator and inhibitor concentration and their efficiencies.

In non-isothermal conditions the induction time may be calculated as the sum of the contributions in each isothermal temperature step. Then the non-isothermal induction time may be calculated by:

$$\Theta = \int_0^{t_i} K_{ti} \exp\left(- \frac{E_d}{RT} \right) dt \tag{7}$$

where Θ is a dimensionless parameter ranging from 0 to 1. The value $t = t_i$ at which $\Theta = 1$, represents the induction time calculated in non-isothermal conditions. The induction times, measured in different isothermal DSC experiments

were corrected for the sample preparation time using Eq. (7) in a simple two-temperature step case: at 20°C the handling time (t_{hc}) and the delay of the onset of reaction measured by DSC were summed in order to obtain the true t_i. The ratio between t_h and t_i at 20°C was used to correct the induction times observed at the other temperatures. Experimental induction times and the results yielded by Eq. (6) are compared in Fig. 2. The parameters of Eq. (6) are listed in Table 2.

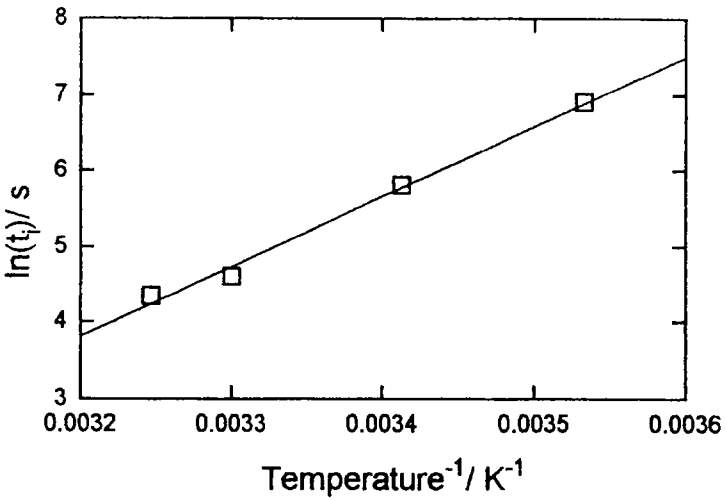

Fig. 2 Temperature dependence of the induction time measured in isothermal DSC experiments

Table 2 Parameters of the kinetic model

Parameter	Value	Parameter	Value
$\ln K_{ti}/s^{-1}$	25.71	$\ln K_{do}/l\ mol^{-1}s^{-1}$	21.78
$(E_d\ R)/K$	9223		
n	0.7	a	–0.1336
m	0.86	b/K^{-1}	0.00307
$\ln K_o/s^{-1}$	18.8	$(E_a/R)/K$	6600

The measurement of the induction time may be used for the calculation of the constant K_d as a function of the temperature using Eq. (4) or Eq. (5) once q and f are known. In the studied case, assuming that q and f assume about the same values before the propagation reaction starts and that the amine and peroxide are present in a stoichiometric ratio, Eq. (5) is applied to the calculation of K_d, using the DSC values of the induction time. The temperature dependence of K_d is shown in Fig. 3 and the parameters in Table 2.

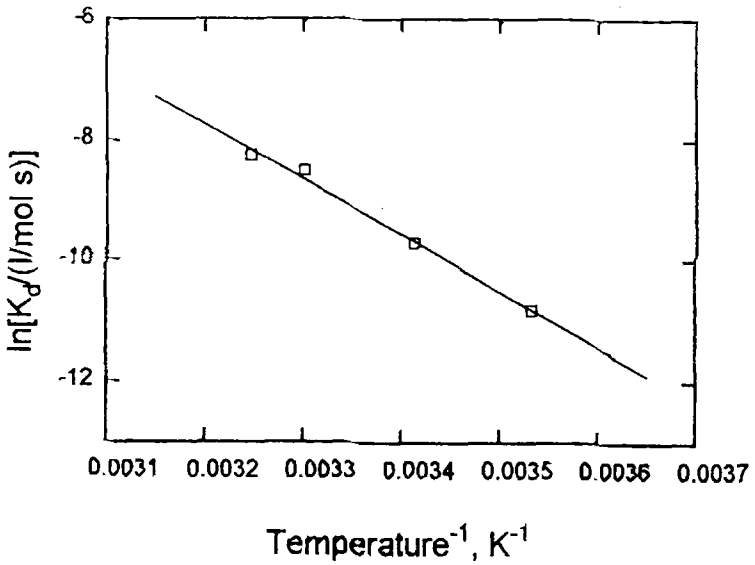

Fig. 3 Temperature dependence of the kinetic constant of the initiator decomposition, K_d

Propagation and termination

DSC measurements may be used for the determination of the advancement of the polymerization by assuming that the heat evolved during the polymerization reaction is proportional to the overall extent of reaction given by the fraction of reactive groups consumed. Following this approach the degree of reaction, α, is defined as:

$$\alpha = Q(t)/Q_{tot} \tag{8}$$

where $Q(t)$ is the partial heat of reaction developed during a DSC experiment and Q_{tot} represents the maximum heat of reaction measured in a non-isothermal experiment, taken as a reference values. The reaction rate, $d\alpha/dt$, is thus obtained from the heat flow dQ/dt as:

$$d\alpha/dt = 1/Q_{tot}(dQ/dt) \tag{9}$$

A value of $Q_{tot} = 125$ J g^{-1} is assumed as an average of the heats of reaction measured in non-isothermal experiments. It must be noted that his value, if referred to the weight of MMA, is lower (375 J g^{-1}) than the theoretical heat of polymerization of MMA (550 J g^{-1}). This can be explained by assuming that the liquid monomer is an oligomer rather then pure MMA. The use of an oligomer reduces the heat of polymerization and hence the maximum peak temperature in the cement.

The kinetics of propagation is dominated by the autoacceleration effect. The theoretical expression for steady state polymerization before autoacceleration occurs is:

$$\frac{d\alpha}{dt} = k_p\left(\frac{2fk_d}{k_t}\right)^{0.5}(1-\alpha) \tag{10}$$

In Eq. (10) kp and kt represent the kinetic constants of the propagation and termination reactions. In accordance with Eq. (10), a first order kinetics should be observed before autoacceleration occurs [9]. This behaviour is not detected for the polymerization of the studied material. This result is in agreement with the data of High et al. [9]. They measured the time to the onset of autoacceleration of MMA as a function of increasing amount of added PMMA to the monomer up to a concentration of 30% by weight of polymer. The concentration of predissolved PMMA in monomer, capable of inducing autoacceleration at zero time, obtained according to the data of High *et al.* [9] by an extrapolation procedure, is equal to 63.4%. This value is very close to the concentration of PMMA and copolymer PMMA-PS present in the studied bone cement.

Therefore the assumption of steady state condition in no longer valid, and thus Eq. (10) cannot be applied. The rate of reaction can be expressed as a function of the radical concentration, $[R]$:

$$\frac{d\alpha}{dt} = k_p(1-\alpha)[R] \tag{11}$$

$[R]$ is a function of the ratio of the rates of the initiation and termination reactions. The rate constant of termination decreases in correspondence to the onset of autoacceleration by 3 orders of magnitude, as reported by Sack *et al.* [10]. On the other hand, the rate of initiation, depending essentially on the concentration of initiator and its efficiency, presents a much lower decrease, at least at the beginning of the reaction. Since the onset of autoacceleration occurs for very low values of α, an apparent autocatalytic behaviour is detected at the beginning of the reaction, as clearly shown by the shape of the DSC reaction peak of Fig. 1. Equation 11 may be modified by introducing the dependence of the rate of reaction on α:

$$\frac{d\alpha}{dt} = k'(1-\alpha)\alpha''' \tag{12}$$

Although this expression has a functional shape similar to the DSC curves, it predicts a final degree of reaction equal to 1. This is not in agreement with the experimental data measured by DSC. In fact, the heat developed during iso-

thermal DSC experiments (Q_{is}) is lower than Q_{tot}, indicating that a residual reactivity can be still developed. This result can be explained by taking into account the effect of diffusion occurring at high degrees of reaction [2, 13, 15]. The glass transition temperature, continuously increasing during cure, may approach the isothermal cure temperature, strongly reducing the molecular mobility. At this stage of the reaction, the transition to a glassy state (vitrification) strongly affects the polymerization kinetics by reducing the mobility of monomers and radicals whose efficiency goes to zero [10]. When the vitrification occurs, the reaction becomes diffusion controlled and the termination step of the polymerization is governed by this strong reduction in molecular mobility. Under these conditions, the kinetic constant of the propagation reaction, the radical efficiency and, consequently, the overall rate of reaction decrease to zero for a value of α lower than 1. This kinetic behaviour may be modelled using a simple pseudo-autocatalytic expression, obtained by modifying a kinetic equation previously proposed for free-radical polymerization of unsaturated polyester and acrylic thermosetting resins [5, 13]:

$$d\alpha/dt = K\alpha^m(\alpha_m - \alpha)^n (1 - \alpha) \tag{13}$$

where m and n are positive fitting parameters not dependent on temperature, and K is a single temperature-dependent rate constant given by an Arrhenius-type equation:

$$K = K_o \exp(-E_a/RT) \tag{14}$$

K_o is the pre-exponential factor, R is the gas constant, E_a the activation energy and T the absolute temperature. In Eq. (13) the maximum degree of reaction, α_m is introduced:

$$\alpha_m = Q_{is}/Q_{tot} \tag{15}$$

The temperature dependence of α_m, shown in Fig. 4, can be well represented by a linear relationship [13, 15]:

$$\alpha_m = a + bT \text{ for } T < T_{gmax}; \quad \alpha_m = 1 \text{ for } T > T_{gmax} \tag{16}$$

When the temperature approaches the glass transition temperature (T_g) of the fully polymerized system (T_{gmax}), $\alpha_m = 1$. The fitting parameters a and b are given in Table 2.

Introducting the term $(\alpha_m - \alpha)^n$, Eq. (13) correctly predicts that the rate of reaction goes to zero when α approaches the limiting value α_m.

The overall kinetic behaviour under isothermal conditions is studied by uncoupling the initiator-inhibitor reaction and the polymerization reaction. The induction time is calculated from the time $t=0$ by Eq. (6) or (7), and sub-

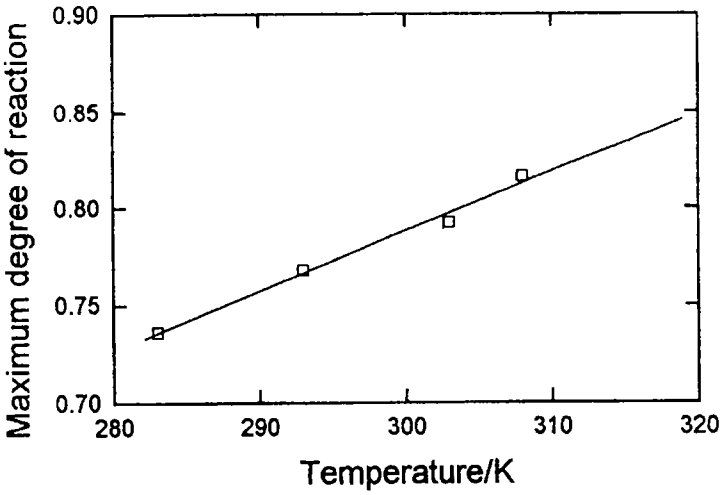

Fig. 4 Temperature dependence of the maximum degree of reaction obtained from isothermal DSC polymerization experiments

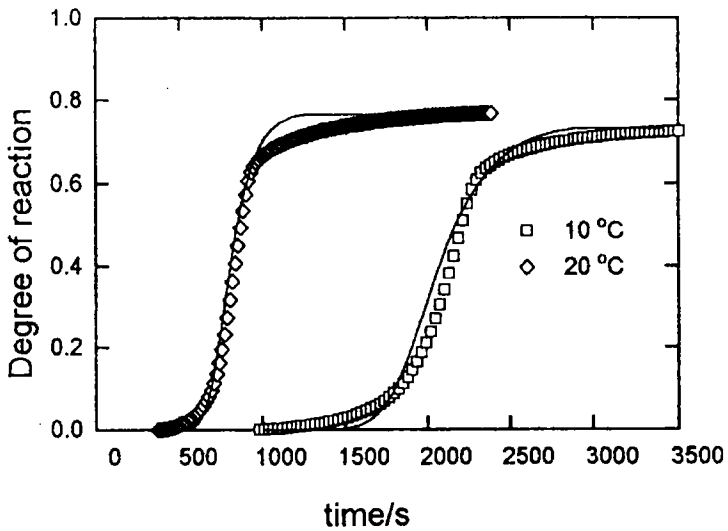

Fig. 5 Comparison between kinetic model predictions and experimental degree of reaction data under isothermal conditions

sequently the evolution of the degree of reaction is obtained by integrating Eq. (13). Therefore the initial condition for Eq. (13) is given by:

$$t = t_i \qquad \alpha = 0 \tag{17}$$

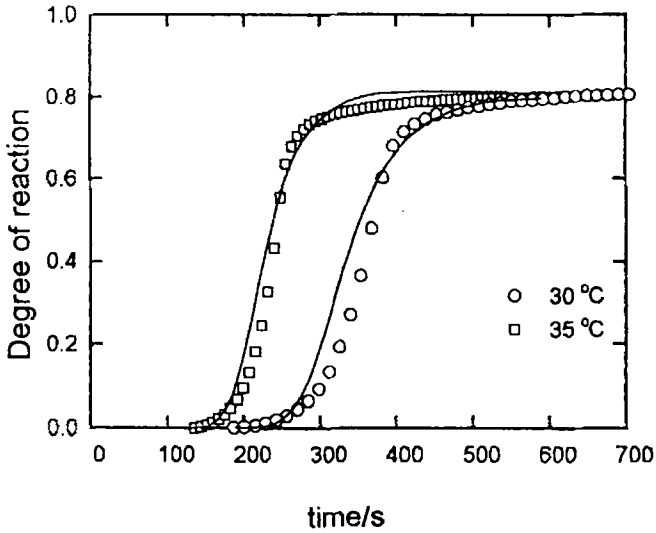

Fig. 6 Comparison between kinetic model predictions and experimental degree of reaction data under isothermal conditions

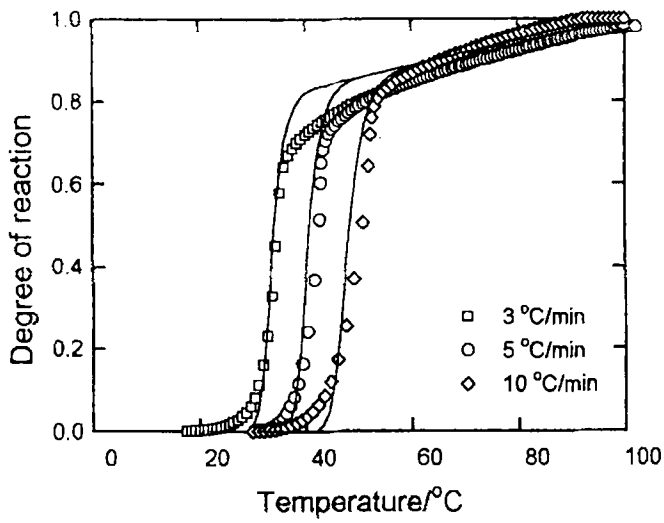

Fig. 7 Comparison between kinetic model predictions and experimental degree of reaction data under non-isothermal conditions

The ability of the model to represent the polymerization kinetics of the studied bone cement at four polymerization temperatures is demonstrated in Figs 5 and 6. The values of the kinetic parameters of the model, evaluated by regression analysis, are listed in Table 2.

In order to verify the model under non-isothermal conditions, the induction time is calculated from Eq. (7). Equation (7), representing the reaction between inhibitor and initiator for the entire set of thermal conditions is integrated before the propagation reaction starts (Eqs (13–17)). The numerical integration of Eq. (7), performed using an explicit method, is performed taking $t=0$ in correspondence to the contact between initiator and monomer, taking into account the mixing and handling time. Comparison of experimental data with model predictions under non-isothermal conditions is shown in Fig. 7. The good agreement observed in Figs 5–7 indicates that the presented simple model can be used to represent the described complex kinetic behaviour.

Integration of the kinetic model

The integration of Eq. (13) with the initial condition given by Eq. (17) is performed using a second-order Runge-Kutta method.

However the integral of Eq. (13) cannot be obtained with the given initial condition for every value of the parameter m. The analytical solution of Eq. (13) could be obtained by separating the variables:

$$\int_0^{\alpha} \frac{d\alpha}{\alpha^m(\alpha_m - \alpha)^n(1 - \alpha)} = \int_{t_i}^{t} K dt \tag{18}$$

Under isothermal conditions the second term is easily integrated while the first term cannot be analytically integrated. Nevertheless, in a small interval close to $t=t_i$, α goes to zero and in Eq. (18) the terms $(1-\alpha)$ and $(\alpha_m-\alpha)^n$ may be approximated by 1 and α_m^n, respectively:

$$\int_0^{\alpha} \frac{d\alpha}{\alpha^m} = K\alpha_m^n (t - t_i) \tag{19}$$

The analytical integration of the first term for $m\neq1$ leads to:

$$\left[\frac{1}{1 - m} \alpha^{1-m}\right]_0^{\alpha} = K\alpha_m^n(t - t_i) \tag{20}$$

This integral may be calculated at the point where $\alpha=0$ only if m is lower than 1. For $m>1$ the first term goes to infinity at $\alpha=0$. The case of $m<0$ must be excluded in order to keep Eq. (13) suitable for the modelling of the observed pseudo-autocatalytic behaviour. For $m=1$ the integral of Eq. (19) is:

$$[\ln\alpha]_0^{\alpha} = K\alpha_m^n(t - t_i) \tag{21}$$

In this case, the first term goes to infinity at $\alpha=0$. This analytical treatment is confirmed by the results of the numerical integration (reported below) performed don Eqs 13–17 under isothermal and non-isothermal conditions.

The numerical integration of Eq. (13) with the initial conditions given by Eq. (17) is obtained using a second-order Runge-Kutta method. However, after the induction time is consumed according to Eq. (7), Eq. (13) must be integrated by calculating a value of $\alpha\neq0$ for the first time interval. Before starting with the integration of the model this value is determined for a time interval, Δt, using the following routine: a tentative small value of α_1 (10^{-4} or so) is assigned to α and a first value of the degree of conversion α_2 is calculated according to the following iterative routine repeated for $i=1$ to n_c:

$$(d\alpha/dt)_i = f(\alpha_i) \tag{22}$$

$$\alpha_{i+1} = (d\alpha/dt)_i \Delta t \tag{23}$$

At each step the convergence of the routine is checked for a given tolerance E:

$$\left| \frac{\alpha_{i+1} - \alpha_i}{\alpha_i} \right| < E \tag{24}$$

If the error is higher than E, the cycle is repeated by increasing i by one unit, otherwise the routine is arrested for $i=n_c$ and the initial value, α_{nc}, is assumed for the subsequent Runge-Kutta method. In practice, convergence is obtained if the function $\alpha(t)$ may be considered linear, within an error E, between $t=t_i$ and $t=t_i+\Delta t$. In Tables 3–5 the effect of different values of α_1, E and Δt on the convergence values, α_{nc}, is presented. The values reported in these tables are calculated using the parameters of Table 2 at a constant temperature of 20°C. As shown in Table 3, the use of different initial values of α_1 has no effect on α_{nc}. A decrease in E is reflected in lower values of α_{nc} converging toward a constant value (Table 4). As can be expected, as shown in Table 5, α_{nc} is significantly affected by Δt. The convergence of the routine to a finite value α_{nc} is obtained only for $0<m<1$ as predicted by Eqs (20–21).

Table 3 Effect of α_1 on the convergence value α_{nc} ($E=10^{-4}$, $\Delta t=0.2$ s and $T=20$°C)

α_1	α_{nc}
10^{-1}	$7.43\cdot10^{-18}$
10^{-3}	$7.43\cdot10^{-18}$
10^{-6}	$7.43\cdot10^{-18}$

Table 4 Effect of E on the convergence value α_{nc} ($\alpha_1 = 10^{-3}$, $\Delta t = 0.2$ s and $T = 20°C$)

E	α_{nc}
10^{-1}	$1.10 \cdot 10^{-17}$
10^{-2}	$7.70 \cdot 10^{-18}$
10^{-3}	$7.45 \cdot 10^{-18}$
10^{-4}	$7.43 \cdot 10^{-18}$
10^{-6}	$7.43 \cdot 10^{-18}$

Table 5 Effect of Δt on the convergence value α_{nc} ($\alpha_1 = 10^{-3}$, $E = 10^{-3}$ and $T = 20°C$)

Δt	α_{nc}
0.002	$3.86 \cdot 10^{-32}$
0.02	$5.36 \cdot 10^{-25}$
0.2	$7.43 \cdot 10^{-18}$
2	$1.04 \cdot 10^{-10}$
20	$1.40 \cdot 10^{-3}$

Conclusions

In this work the reactive behaviour of an MMA based commercial bone cement was studied. The reaction kinetics is analysed using a simple phenomenological model accounting for the effects of autoacceleration and vitrification on the propagation and termination steps of the polymerization, respectively. The presence of the inhibitor is taken into account by introducing a characteristic time for the reaction between initiator and inhibitor (the induction time) that can be detected in DSC experiments. The induction time is applied to a rough evaluation of the kinetic constant of the decomposition of the initiator. A good agreement was found between experimental data and model results under isothermal and non-isothermal conditions. The analytical and numerical details related to the integration of the model are discussed, highlighting the limits for the parameter m related to the imposed initial condition.

* * *

The author would like to thank Prof. L. Nicolais, Prof. G. Guida and R. L. Torre from the University of Naples 'Federico II' and Prof. J. M. Kenny from the University of Perugia for their useful advice.

References

1 G. M. Brauer, D. R. Steinberger and J. W. Stansbury, J. Biomed. Mater. Res., 20 (1986) 839.

2 G. Odian, Principles of polymerization, McGraw-Hill,New York,1988.
3 I. Mita and K. Horie, JMS-Rev. Macromol. Chem Phys., C27(1) (1987) 91.
4 J. M. Kenny, A. Maffezzoli and L. Nicolais, Compos. Sci. Tech., 38 (1990) 339.
5 A. Maffezzoli, R. Terzi and L. Nicolais, J. Mater. Sci.: Mater. in Medicine, 6 (1995) 155.
6 S. T. Balke and A. E. Hamielec, J. Appl. Polym. Sci., 17 (1973) 905.
7 J. M. Dionisio and K. F. O'Driscoll, J. Polym. Sci: Polym. Chem., 18 (1980) 241.
8 H. K. Mahabadi and K. F. O'Driscoll, Macromolecules, 10 (1977) 55.
9 K. A. High, H. B. Lee and D. T. Turner, Macromolecules, 12 (1979) 332.
10 R. Sack, G. V. Schulz and G. Meyerhoff, Macromolecules, 21 (1988) 3345.
11 A. Maffezzoli, D. Ronca, G. Guida, I. Pochini and L. Nicolais, submitted for publication on J. Mater. Sci.: Mater in Medicine.
12 A. Maffezzoli, R. Terzi and L. Nicolais, J. Mater. Sci.: Mater. in Medicine, 6 (1995) 161.
13 J. D. Fan and L. J. Lee, Polym. Compos., 7 (1986) 250.
14 J. M. Kenny and A. Trivisano, Polym. Eng. Sci., 31 (1991) 1426.